ACS APPLIED MATERIALS & INTERFACES

Research Article

www.acsami.org

Functionalized PDMS with Versatile and Scalable Surface Roughness Gradients for Cell Culture

Bingpu Zhou,[†,§] Xinghua Gao,[‡] Cong Wang,[†] Ziran Ye,[§] Yibo Gao,[∥] Jiao Xie,[⊥] Xiaoxiao Wu,[§] and Weijia Wen*[,†,‡,§,∥,⊥]

[†]Nano Science and Technology Program and KAUST-HKUST Micro/Nanofluidic Joint Laboratory, [§]Department of Physics, and [∥]Environmental Science Programs, School of Science, The Hong Kong University of Science and Technology, Clear Water Bay, Kowloon, Hong Kong

[‡]Biomedical Research Institute, Shenzhen Peking University–The Hong Kong University of Science and Technology Medical Center, Shenzhen, People's Republic of China

[⊥]The Soft Matter and Interdisciplinary Research Institute, College of Physics, Chongqing University, Chongqing, China

ABSTRACT: This manuscript describes a simple and versatile approach to engineering surface roughness gradients via combination of microfluidics and photopolymerization. Through UV-mediated polymerization, *N*-isopropylacrylamide with concentration gradients are successfully grafted onto PDMS surface, leading to diverse roughness degrees on the obtained PDMS substrate. Furthermore, the extent of surface roughness can be controllably regulated via tuning the flow rate ratio between the monomer solution and deionized water. Average roughness ranging from 2.6 ± 0.7 nm to 163.6 ± 11.7 nm has been well-achieved in this work. Such PDMS samples are also demonstrated to be capable of working as supporting substrates for controlling cell adhesion or detachment. Because of the different degrees of surface roughness on a single substrate, our method provides an effective approach for designing advanced surfaces for cell culture. Finally, the thermosensitive property of *N*-isopropylacrylamide makes our sample furnish as another means for controlling the cell detachment from the substrates with correspondence to the surrounding temperature.

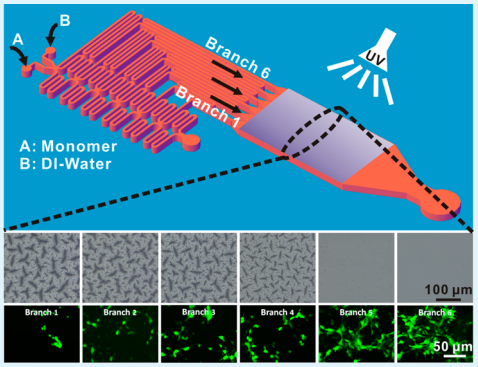

KEYWORDS: *microfluidics, roughness gradients, PDMS, N-isopropylacrylamide, cell culture*

1. INTRODUCTION

Over the past decades, it has been well-demonstrated that the microenvironment in which cells reside plays a pivotal role in regulating a variety of cellular behaviors such as adhesion, differentiation, migration, etc.[1−4] Apart from the biochemical signals of the extracellular matrix (ECM),[5,6] cells have also been recognized to be capable of reacting to the physical nature of the underlying substrates,[7,8] e.g., the mechanical stiffness, topographic features, or surface roughness.[9,10] Thanks to the rapid progress in micro/nanofabrication approaches, nowadays researchers can engineering or synthesize custom-designed substrates. Such synthetic microenvironments provide advantageous opportunities for investigators to figure out the interactions between the physical environment and the cellular behaviors.[11,12]

Surface roughness, which commonly relates to the texture of the uppermost layer of a bulk material, is one of the most important physical factors that influence cell functions. To date, several kinds of approaches have been developed to produce controlled surface roughness including nanoparticle/nanofiber formation,[13] surface grafting,[14] chemical processing,[15] etc. It has also been indicated from extensive evidence that the roughness degree of the supporting substrate can effectively manipulate a host of cellular behaviors, e.g., proliferation[16] and osteointegration.[17] Particularly, roughness gradients on one substratum are typically more favorable, as they enable systematic investigations performed within a single experiment while preserving varying surface parameters.[18−20] For instance, by a two-step roughening and smoothening process, T. P. Kunzler et al. have found that the proliferation of human gingival fibroblasts (HGF) decreased with increasing roughness on one substrate.[16] Recently, roughness gradients of polycaprolactone were designed via A. B. Faia-Torres et al. as a platform to identify the impact of roughness on osteogenic fate of stem cells in vitro.[21] Even though systematic studies have been performed on account of surface roughness gradients, it has yet been limitedly focused on the flexible modulation of roughness degrees in a straightforward manner. The capability to alter average roughness (R_a) of the substrate for cell culture facilitates a simple approach to search for optimal testing parameters within minimum time consumption. In regard of this, here we present a novel method via combination of

Received: May 10, 2015
Accepted: July 21, 2015
Published: July 21, 2015

DOI: 10.1021/acsami.5b04032
ACS Appl. Mater. Interfaces 2015, 7, 17181−17187

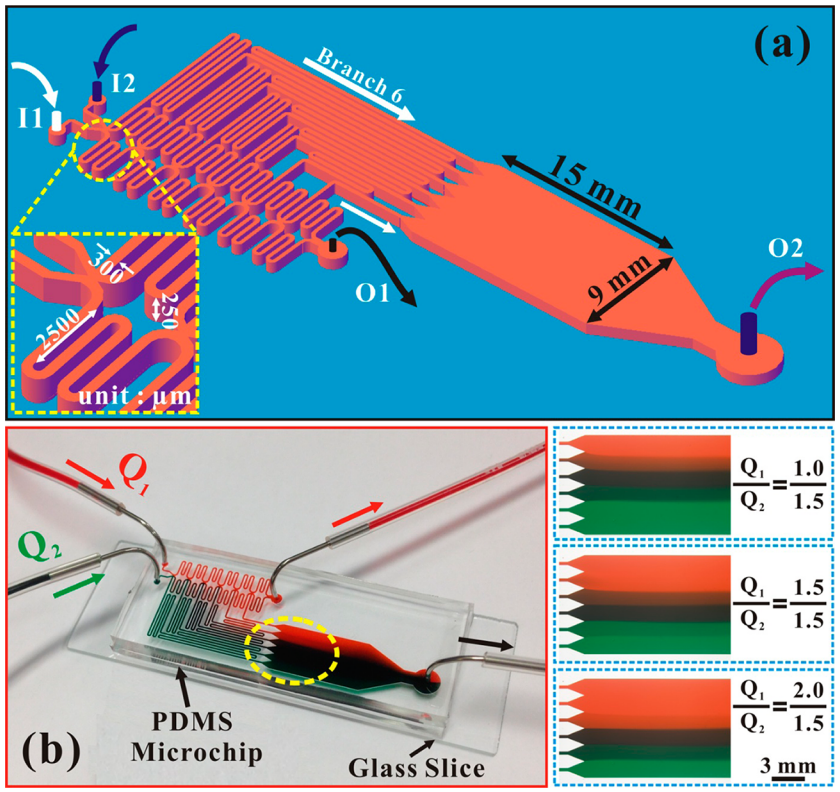

Figure 1. (a) 3D configuration of microfluidic chip for concentration gradient generation with six branches. The branches were combined together close to the outlet O2 as a collection chamber. (b) Fabricated microfluidic chip with injected green/red ink solutions for better contrast. The bottom right figure provides the tunable concentration gradients in six branches via changing the values of Q_1/Q_2 as described.

microfluidics and photopolymerized grafting to flexibly restructure surface roughness gradients on native Polydimethylsiloxane (PDMS) surface.

Up to now, microfluidics has been extensively demonstrated as a powerful means for generation of chemical concentration gradients.[22−24] As presented in our previous work, concentration gradients can be simply established via a microfluidic network and each particular concentration can be flexibly tuned via changing the flow rates between two incoming microstreams.[25] Here, such microfluidic design is employed to build concentration gradients of *N*-isopropylacrylamide (NIPAM) in microchannels, which will then be grafted onto native PDMS surface via photopolymerization. NIPAM is a thermoresponsive polymer that has been well-established and adopted in all sorts of biological aspects such as protein adsorption and cell manipulation.[26−28] NIPAM is of great interest for its reversible conformational transition from expanded coil to compact globule related to the temperature change around the lower critical solution temperature (LCST) of 32 °C, which is in a physiologically relevant temperature range.[29,30] In this report, we will demonstrate that not only the surface roughness gradients could be used to systematically figure out the relationships between cell behaviors and substrate morphologies but the change in ambient temperature can also facilitate regulating cell adhesion or detachment from the supporting substrates.

2. METHODS

Figure 1a shows the configuration of our microfluidic network design for generation of controllable concentration gradients. The fabrication process of PDMS-based microfluidic device follows conventional soft-lithography technique and replica molding method.[31,32] As shown in the figure, I1 and I2 are inlets for injections of solutions with different concentrations, whereas O1 and O2 are outlets for solution exports. Both inlets were connected with individual syringe pump (PHD 2000, Harvard Apparatus, Holliston, USA) such that the flow rates could be adjusted separately. Design principle of the concentration gradient generator has been previously discussed in detail in our previous work.[25] The basic principle of the gradient generator lies in diffusion and convection during liquid transports inside the microchannel. Via changing the flow rates of two inlets (Q_1 and Q_2 for I1 and I2, respectively), the localized concentration in each branch can be promptly adjusted due to the redistribution of the flows inside the microfluidic channel. Key dimensional parameters of a critical part of the microfluidic chip were provided via the inset. The height and the width of the entire microfluidic channel are designed as around 250 and 300 μm, respectively. The collection chamber, where all six branches were combined together, has a total surface area of 15 mm × 9 mm as depicted. Figure 1b provides the image of the real microfluidic device which is placed on a glass slice. The microchannels were injected with red (Q_1) and green (Q_2) dye solutions for a better contrast. To demonstrate the flexible control of concentration gradients, the bottom right picture gives the dye distributions inside the branches which can be simply tuned via regulating the ratios between Q_1 and Q_2. Here the flow rate ratios (Q_1/Q_2) were set of three conditions namely 1.0/1.5, 1.5/1.5, and 2.0/1.5 as presented. The change of color in the collection chamber represents the variation of concentrations inside each branch channel (yellow dashed ellipse in Figure 1b). As a consequence, it can be confirmed that not only can concentration gradients be established via our design but the particular concentration values in each branch can also be flexibly regulated based on the flow settings.

Recently, grafting of polymers onto substrate surfaces has been extensively developed as the subject of numerous experimental studies. Although kinds of polymer materials (e.g., NIPAM, acrylic acid) have been successfully grafted onto various surfaces (e.g., PDMS, nylon), rare reports focused on controllable grafting of polymers with

DOI: 10.1021/acsami.5b04032
ACS Appl. Mater. Interfaces 2015, 7, 17181−17187

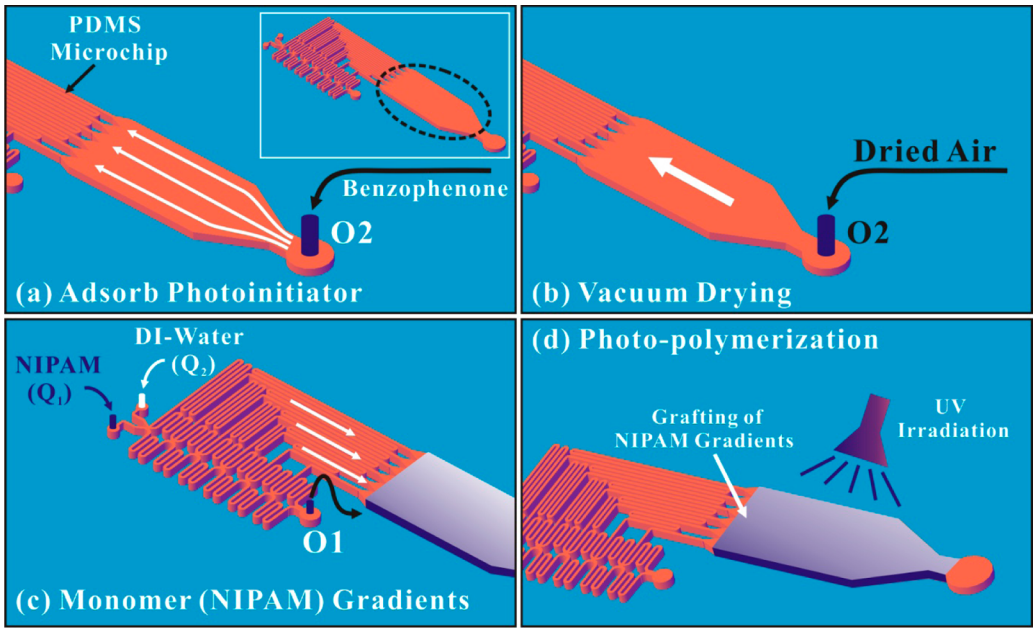

Figure 2. Procedure schematic of grafting NIPAM with concentration gradients onto native PDMS surface via combination of microfluidic approach and post photopolymerization process. (a) Injection of photoinitiator (benzophenone) dissolved in acetone into the microfluidic chip for photoinitiator absorption; (b) microfluidic chip was vacuumed dried for residual removal; (c) generation of monomer (NIPAM) concentration gradients in the collection chamber; (d) photopolymerization to graft NIPAM onto the native PDMS surface with concentrated gradients.

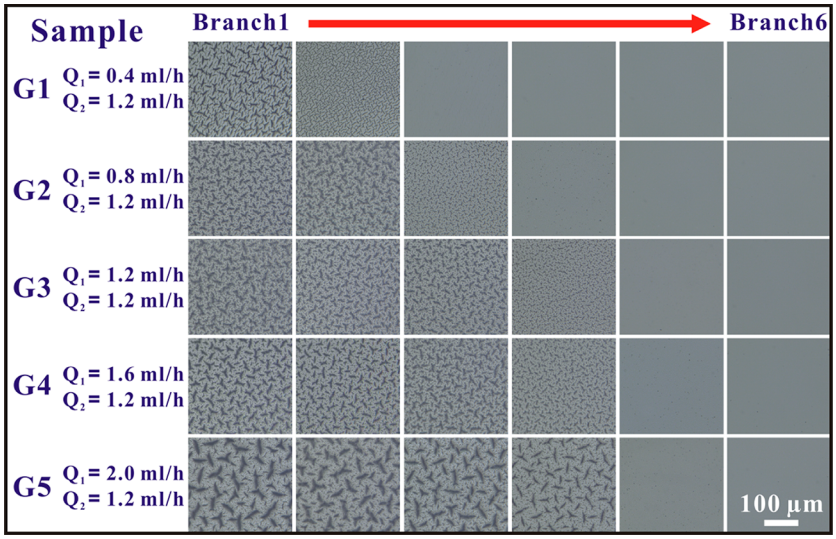

Figure 3. Optical images of PDMS surface grafted with NIPAM concentration gradients. Five samples were demonstrated with tunable Q_1 and fixed Q_2. Branch 1 is the branch with highest NIPAM concentration and branch 6 corresponds to the one of lowest NIPAM concentration.

concentration gradients.[33−35] Figure 2 depicts the preparation procedure of grafting NIPAM with concentration gradients onto native PDMS surface. First, a PDMS slab patterned with microfluidic structures was bonded to another flat PDMS slab after 2 min oxygen plasma cleaning. Prior to the injection of NIPAM solutions, benzophenone (10 wt % in acetone) was flushed through the assembled microchannel via port O2 with a constant flow rate of 5.0 mL/h for 10 min. By this means, hydrophobic benzophenone molecules can be freely adsorbed into the microfluidic PDMS inner-walls thanks to the acetone-induced swelling of PDMS matrix.[36,37] The whole microfluidic system was then vacuum-dried for ∼10 min to remove residual solvents from the microfluidic channel. Monomer solution (20 wt % NIPAM in DI water) and DI water were then injected simultaneously into the microchannel via I1 and I2, respectively. As described in Figure 1, stable but tunable concentration gradients could thus be flexibly established via regulating the ratios between two incoming flow rates. It can be thus achieved that the NIPAM concentrations will gradually increase from branch 6 to branch 1. For a typical condition of Q_2/Q_1, we waited for 5 min to ensure the stable establishment of concentration gradients inside the collecting chamber. Afterward, injection was stopped and the microfluidic device was immediately moved onto an ice-pack and irradiated under ultraviolet light for 15 min, with a fixed distance of ∼10 cm between the UV lamp (50 mW/cm^2) and the microfluidic sample. Upon such UV-mediated polymerization process, NIPAM can be successfully grafted onto the uppermost layer of the bulk PDMS substrate. Finally, the NIPAM-grafted PDMS slab was gently detached from the microfluidic assembly and sequentially flushed with ethanol and DI water to completely remove residuals.

DOI: 10.1021/acsami.5b04032
ACS Appl. Mater. Interfaces 2015, 7, 17181−17187

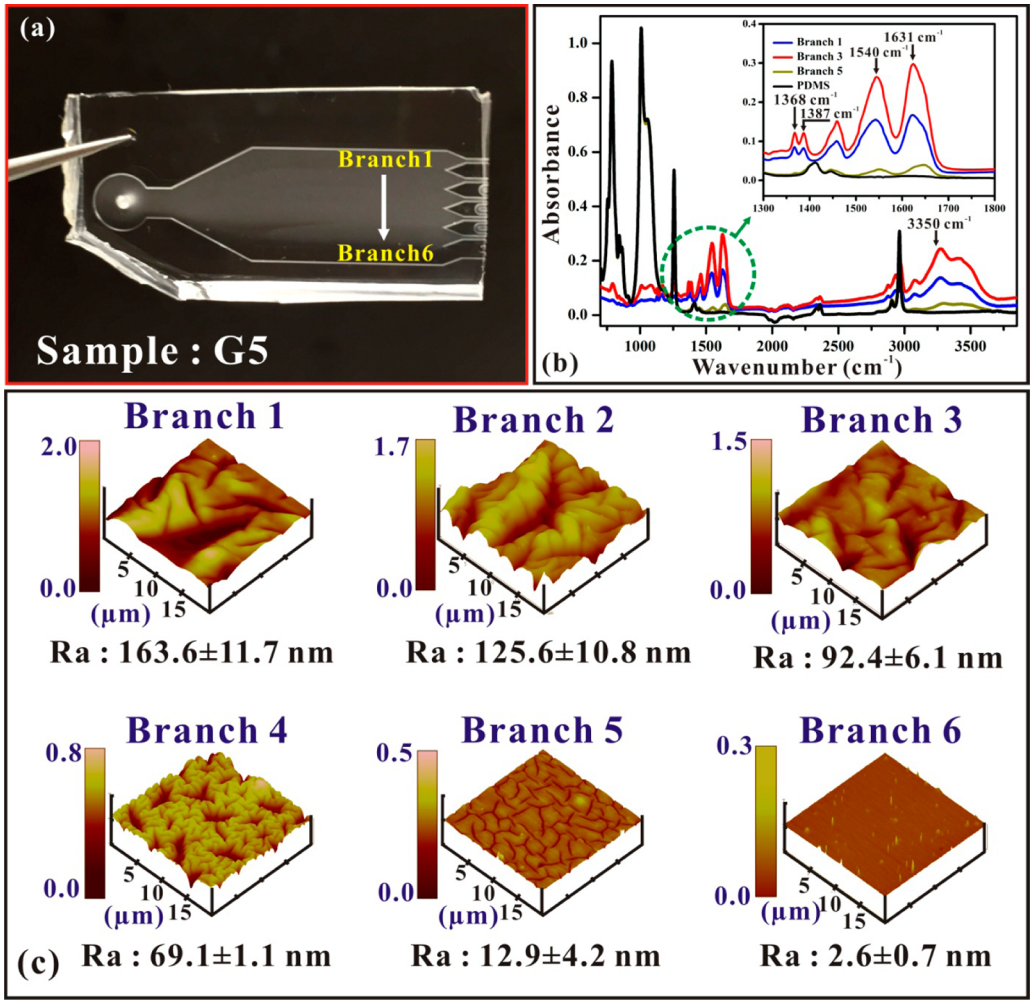

Figure 4. (a) Optical image of the obtained PDMS sample G5 grafted with NIPAM concentration gradients; (b) FTIR spectra of NIPAM gradients-grafted PDMS compared to native PDMS. Three branches (branch 1, 3, and 5) from sample G5 (indicated in panel a) were selected for spectral measurement. (c) AFM images of the six branches from sample G5. All of the AFM images were obtained in ambient conditions with scan area of $(20\ \mu m)^2$. The average roughness degrees of the six selected regions were found to be 163.6 ± 11.7 nm, 125.6 ± 10.8 nm, 92.4 ± 6.1 nm, 69.1 ± 1.1 nm, 12.9 ± 4.2 nm, and 2.6 ± 0.7 nm, respectively.

3. RESULTS AND DISCUSSIONS

3.1. Surface Characterization. As mentioned above, the exact concentration in each branch can be flexibly tuned via changing the flow rate ratios. Here, we fixed the flow rate of DI water (Q_2) while gradually changed the flow rate of the monomer solution (Q_1) for tuning the specific concentrations in each branch. Q_2 was set as 1.2 mL/h and Q_1 gradually increased from 0.4 to 2.0 mL/h with a step of 0.4 mL/h. For each condition, the obtained sample was named as G1, G2, and so forth, where G1 stand for sample with Q_1 of 0.4 mL/h and Q_2 of 1.2 mL/h (as described in Figure 3). For each sample, branch 1 corresponds to the branch with highest NIPAM concentration and branch 6 corresponds to the one with lowest concentration. Figure 3 shows the optical images of the PDMS surface where NIPAM has been grafted with gradients. It can be obviously found that the feature size of the investigated surface gradually decreased from branch 1 to 6 with consistence to the concentration gradients of NIPAM. By this means, it can be concluded that the NIPAM concentration plays an important role in defining the surface morphologies of PDMS. In addition, via tuning the flow rate ratios, we could also obtain different feature sizes of different samples even within the same branch. For example, the feature size of branch 1 from sample G5 is apparently larger than that from sample G3 due to the relative high concentration of NIPAM in this branch before photopolymerization. Typically, a higher Q_1/Q_2 will render a higher NIPAM concentration in the specific branch, such that the feature size of the surface can be found increased as shown in Figure 3.

To confirm the successful grafting of NIPAM onto PDMS surface, Fourier transform infrared spectrometer (FTIR) was introduced for surface composition analysis with a resolution of 2 cm^{-1}. Figure 4a gives the optical images of the obtained PDMS sample G5 with grafted NIPAM gradients. Such sample has been cut from the microfluidic channel for further investigation and experiment. Figure 4b shows the FTIR spectra of PDMS surface grafted with NIPAM gradients compared with native PDMS sample. Without loss of generality, here branches 1, 3, and 5 from sample G5 were chosen for qualitative measurement. Compared to the unmodified PDMS (reference spectrum), the N−H stretch at 3350 and 1540 cm^{-1} as well as C═O stretch at 1631 cm^{-1} confirmed the presence of amide groups in the PDMS surface grafted with NIPAM.[34] Furthermore, the characteristic

DOI: 10.1021/acsami.5b04032
ACS Appl. Mater. Interfaces 2015, 7, 17181−17187

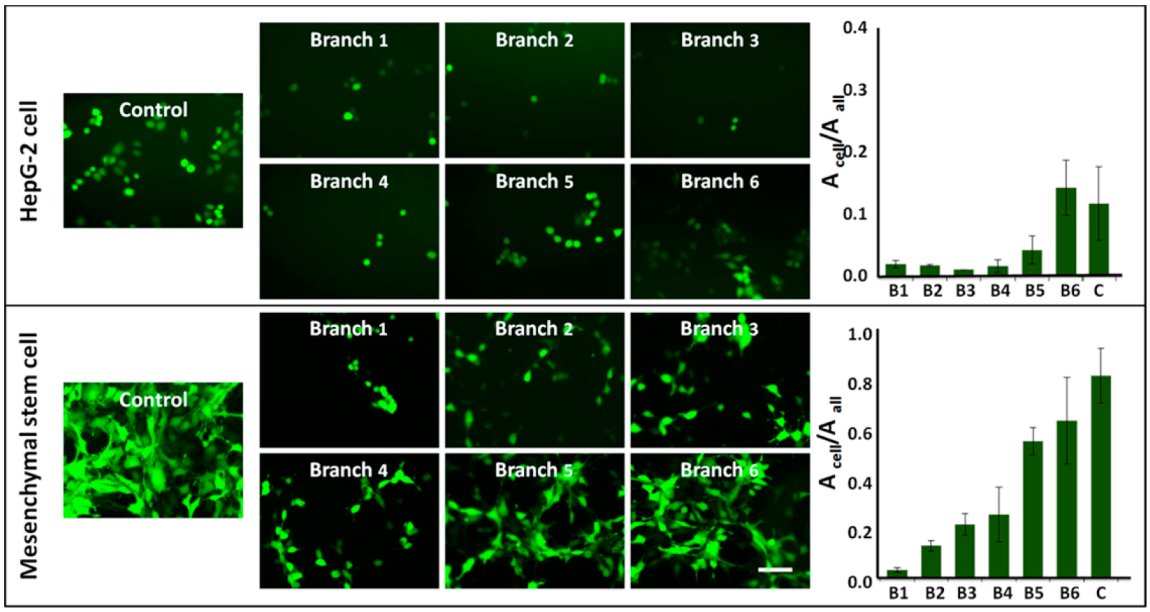

Figure 5. Fluorescence images of cell attachment on the surface with different roughness degrees. HepG-2 cell were stained by cell tracker dye (Green). MSCs were transfected with GFP (green). A_{cell} is utilized to define the total area of cell adhesion, whereas A_{all} as the total area of the vision. The scale bar is 50 μm.

absorption bands at 1368 and 1387 cm^{-1} indicated that the isopropyl groups existed in the scanned regions of the sample. It should be noted that a higher concentration of NIPAM does not exactly render a higher absorbance phenomena in the FTIR spectrum as observed. One possible explanation should be that the flatness of the measured surface also play an important role of the relative intensities of the absorbance. Surface topography of sample G5 was examined via atomic force microscopy (AFM) as found in Figure 4c with a scan area of $(20\ \mu m)^2$. Figure 4c provides typical AFM images of the six branches from sample G5. The average surface roughness (Ra) for the measured positions was 163.6 ± 11.7 nm, 125.6 ± 10.8 nm, 92.4 ± 6.1 nm, 69.1 ± 1.1 nm, 12.9 ± 4.2 nm, and 2.6 ± 0.7 nm, respectively. From the results, we could simply find that the successful grafting of NIPAM gradients results in different roughness degrees of the PDMS surface. In addition, it can be concluded that the roughness degrees gradually decreased from the branch related to higher NIPAM concentration to the branch of lower NIPAM concentration.

3.2. Cell Culture on Sample G5. In this section, sample G5 will be introduced as the supporting substrate for cell culture to demonstrate the impact of roughness degrees on the cellular behaviors. Mesenchymal stem cells (MSCs) derived from mouse bone marrow and Hepatocellular carcinoma cell lines HepG-2 were adopted in this demonstration. The MSCs and HepG-2 cells were maintained in Alpha-MEM (minimum essential medium) and high glucose DMEM (Dulbecco's modified eagle's medium) with 10% fetal bovine serum (FBS), 100 U/ml penicillin, 100 μg/mL streptomycin at 37 °C in a humidified atmosphere containing 95% air and 5% CO_2, respectively. To trace the live cell, the MSCs have been transfected with GFP (green fluorescent protein), whereas HepG-2 cells were stained by Cell Tracker Probes Green CMFDA (5-chloromethylfluorescein diacetate). Furthermore, the cell F-actin has also been stained with Alexa Fluor 488 phalloidin in order to characterize the cell morphology on the PDMS substrate. The MSCs were obtained from Dalian Institute of Chemical Physics, Chinese Academy of Sciences, China and the HepG-2 cells were purchased from ATCC. The cell culture medium (Alpha-MEM and high glucose DMEM), FBS, penicillin, streptomycin were obtained from GIBCO Invitrogen. The Cell Tracker Probes Green CMFDA and the Alexa Fluor 488 phalloidin were purchased from Life Invitrogen. All the cell staining processes were following standard product instructions. Cells were visualized using Olympus fluorescence microscopy (Olympus IX 71, Japan) and the collected images were then analyzed via Image Pro Plus 6.0.

Before each cell culture cycle, the NIPAM-grafted PDMS substrate was soaked in 75% ethanol for half an hour, followed by washing with sterile water and rinsing with Phosphate-Buffered Saline (PBS) for three times. After that, the sample was directly transferred to sterile culture dish and covered with cell culture mediums for further biological experiment. Before the cell seeding process, the above cell culture mediums were completely removed from the PDMS sample and the culture dish. Fresh cell culture mediums with preadjusted cell densities were then provided to the culture dish. MSCs and HepG-2 were respectively seeded onto the PDMS substrate with density of approximately $1 \times 10^5/cm^2$ here. After 24h in the 37 °C incubator, the fluorescence images were recorded and given as Figure 5. Pictures labeled with control are control experiments of cell culture based on native PDMS substrate. It can be observed from the figure that both kinds of cells can attach to the surface of the substrate within the investigated branches. This is consistent with other reports that under such temperature, the NIPAM-grafted surface can be adopted as a substrate for successful cell attachment.[29] However, the number of the attached cells (both HepG-2 and MSCs) obviously differs from each branch as provided by the data in Figure 5. The ratio between the total area of cell adhesion and the captured vision (A_{cell}/A_{all}) was calculated in order to characterize the cell attachment results based on different roughness regions. The right part of Figure 5 gives the values of A_{cell}/A_{all} for all six branches where B1 stands for branch 1 and so forth. The data showed that with the increase of surface roughness, the value of A_{cell}/A_{all} became relatively smaller which indicated

DOI: 10.1021/acsami.5b04032
ACS Appl. Mater. Interfaces 2015, 7, 17181−17187

that fewer cells could be capable to attach well onto such particular region. In addition, from the images we also observed that, with the increase of surface roughness the cell could not freely flatten and spread. It suggested that the number of attached cells as well as the areas of attached cells were both reduced with correspondence to the increase of the degrees of surface roughness.

To characterize the cell morphology on PDMS substrate, the cell F-actin and nucleus were further stained with Alexa Fluor 488 phalloidin and DAPI (4′,6-diamidino-2-phenylindole), respectively. Such processes of cell staining were conducted at room temperature (approximately 20 °C) and the corresponding fluorescence images were shown in Figure 6.

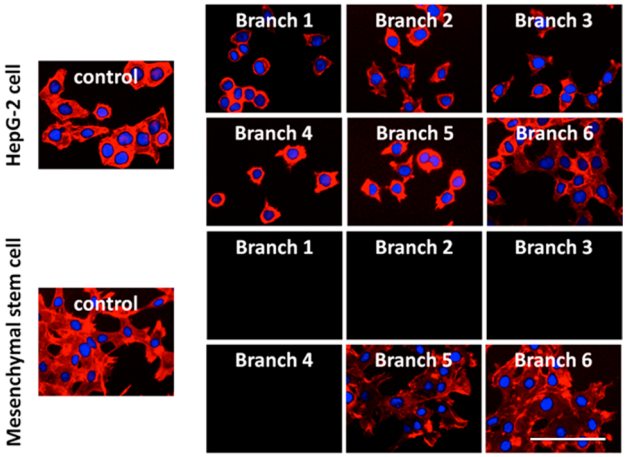

Figure 6. Fluorescence images of cell F-actin on Sample G5. Cell F-actin and nucleus were stained with Alexa Fluor 488 phalloidin (red) and DAPI (blue), respectively. The scale bar is 50 μm.

As NIPAM alone could undergo reversible phase transition in response to the surrounding temperature as mentioned above, grafting of NIPAM makes the obtained PDMS surface (sample G5) temperature sensitive. For such case with temperature of ~20 °C, the surface of the PDMS substrate commonly got swollen due to the presence of NIPAM. Such a change of the surface characteristic would result in obvious cell detachment from the substrate. We observed that with the increase of the grafted NIPAM concentrations, more cells, especially MSCs, could detach from the substrate among branches 1−4, whereas for branches 5 and 6, it was found that most MSCs can still rest on the substrate compared to the other branches. One possible reason for this phenomenon is that for these two branches (branch 5 and 6), relative smaller concentrations of NIPAM were grafted onto the PDMS surface. As a consequence, the temperature change will not result in obvious surface morphology alternation which is required for successful cell detachment. However, for HepG-2 cells, it could be perceived that to some extent portion of the cells could still reside well on the substrate for all six branches under the same condition as MSCs with temperature of around 20 °C. This may be due to the fact that HepG-2 cells do not present an obvious response to the alternation of the supporting substrates, which would finally lead to cell detachment as mentioned above. As a result, the swollen change of the substrate surface will not dramatically affect the attachment results of HepG-2 cells.

4. CONCLUSIONS

In summary, we have successfully grafted NIPAM onto PDMS surface with concentration gradients via combination of microfluidic concentration gradient generators and photopolymerization process, leading to realization of surface roughness gradients in a highly controllable manner. Such a simple and effective method can be adopted to quickly generate substrates with a wide range of surface roughness in nanoscale. The magnitude of the average surface roughness in this work was well controlled within range up to ~163.6 ± 11.7 nm. Via tuning the flow rate ratios between two injecting streams containing NIPAM monomer and DI water, five samples with different extents of roughness values were successfully prepared. Finally, sample G5 was adopted as the substrate for cell culture where the diverse degrees of surface roughness reveal to be playing an important role to define the cell behaviors. It was concluded that the number of attached cells and the areas of attached cell were both reduced with correspondence to the degree increase of surface roughness. We believe that such a versatile approach of engineering surface roughness gradients can be broadly applied in various aspects from tissue engineering to cell investigations.

AUTHOR INFORMATION

Corresponding Author

*E-mail: phwen@ust.hk. Fax: +852 23581652. Tel: +852 23587979.

Notes

The authors declare no competing financial interest.

ACKNOWLEDGMENTS

The authors acknowledge the support by Hong Kong RGC grant HKUST 605411 and NSFC/RGC joint grant N_HKUST601/11. The work was also partially supported by the Special Fund for Agro-scientific Research in the Public Interest, Ministry of Agriculture of the People's Republic of China 201303045 and PhD Start-up Fund of Natural Science Foundation of Guangdong Province (2014A030310422).

REFERENCES

(1) Stevens, M. M.; George, J. H. Exploring and Engineering the Cell Surface Interface. *Science* **2005**, *310*, 1135−1138.
(2) Huang, J.; Grater, S. V.; Corbellini, F.; Rinck, S.; Bock, E.; Kemkemer, R.; Spatz, J. P. Impact of Order and Disorder in RGD Nanopatterns on Cell Adhesion. *Nano Lett.* **2009**, *9*, 1111−1116.
(3) Machida-Sano, I.; Hirakawa, M.; Matsumoto, H.; Kamada, M.; Ogawa, S.; Satoh, N.; Namiki, H. Surface Characteristics Determining the Cell Compatibility of Ionically Cross-linked Alginate Gels. *Biomed. Mater.* **2014**, *9*, 025007.
(4) Naganuma, T.; Traversa, E. The Effect of Cerium Valence States at Cerium Oxide Nanoparticle Surfaces on Cell Proliferation. *Biomaterials* **2014**, *35*, 4441−4453.
(5) Ross, A. M.; Jiang, Z.; Bastmeyer, M.; Lahann, J. Physical Aspects of Cell Culture Substrates: Topography, Roughness, and Elasticity. *Small* **2012**, *8*, 336−355.
(6) Song, W.; Mano, J. F. Interactions between Cells or Proteins and Surfaces Exhibiting Extreme Wettabilities. *Soft Matter* **2013**, *9*, 2985−2999.
(7) Anselme, K.; Davidson, P.; Popa, A. M.; Giazzon, M.; Liley, M.; Ploux, L. The Interaction of Cells and Bacteria with Surfaces Structured at the Nanometre Scale. *Acta Biomater.* **2010**, *6*, 3824−3846.

DOI: 10.1021/acsami.5b04032
ACS Appl. Mater. Interfaces 2015, 7, 17181−17187

(8) Nikkhah, M.; Edalat, F.; Manoucheri, S.; Khademhosseini, A. Engineering Microscale Topographies to Control the Cellesubstrate Interface. *Biomaterials* **2012**, *33*, 5230−5246.
(9) Bettinger, C. J.; Langer, R.; Borenstein, J. T. Engineering Substrate Topography at the Micro- and Nanoscale to Control Cell Function. *Angew. Chem., Int. Ed.* **2009**, *48*, 5406−5415.
(10) Wheeldon, I.; Farhadi, A.; Bick, A. G.; Jabbari, E.; Khademhosseini, A. Nanoscale Tissue Engineering: Spatial Control over Cell-materials Interactions. *Nanotechnology* **2011**, *22*, 212001.
(11) Franco, D.; Klingauf, M.; Bednarzik, M.; Cecchini, M.; Kurtcuoglu, V.; Gobrecht, J.; Ferrari, A. Control of Initial Endothelial Spreading by Topographic Activation of Focal Adhesion Kinase. *Soft Matter* **2011**, *7*, 7313−7324.
(12) Engler, A.; Bacakova, L.; Newman, C.; Hategan, A.; Griffin, M.; Discher, D. Substrate Compliance versus Ligand Density in Cell on Gel Responses. *Biophys. J.* **2004**, *86*, 617−628.
(13) Kotov, N. A.; Winter, J. O.; Clements, I. P.; Jan, E.; Timko, B. P.; Campidelli, S.; Ballerini, L. Nanomaterials for Neural Interfaces. *Adv. Mater.* **2009**, *21*, 3970−4004.
(14) Chung, T. W.; Liu, D. Z.; Wang, S. Y.; Wang, S. S. Enhancement of the Growth of Human Endothelial Cells by Surface Roughness at Nanometer Scale. *Biomaterials* **2003**, *24*, 4655−4661.
(15) Feng, B.; Weng, J.; Yang, B. C.; Qu, S. X.; Zhang, X. D. Characterization of Surface Oxide Films on Titanium and Adhesion of Osteoblast. *Biomaterials* **2003**, *24*, 4663−4670.
(16) Kunzler, T. P.; Drobek, T.; Schuler, M.; Spencer, N. D. Systematic Study of Osteoblast and Fibroblast Response to Roughness by Means of Surface-morphology Gradients. *Biomaterials* **2007**, *28*, 2175−2182.
(17) Elias, C. N.; Oshida, Y.; Lima, J. H. C.; Muller, C. A. Relationship between Surface Properties (Roughness, Wettability and Morphology) of Titanium and Dental Implant Removal Torque. *J. Mech. Behav. Biomed. Mater.* **2008**, *1*, 234−242.
(18) Kim, M. S.; Khang, G.; Lee, H. B. Gradient Polymer Surfaces for Biomedical Applications. *Prog. Polym. Sci.* **2008**, *33*, 138−164.
(19) Wu, J.; Mao, Z.; Tan, H.; Han, L.; Ren, T.; Gao, C. Gradient Biomaterials and Their Influences on Cell Migration. *Interface Focus* **2012**, *2*, 337−355.
(20) Ross, A. M.; Lahann, J. Surface Engineering the Cellular Microenvironment via Patterning and Gradients. *J. Polym. Sci., Part B: Polym. Phys.* **2013**, *51*, 775−794.
(21) Faia-Torres, A. B.; Guimond-Lischer, S.; Rottmar, M.; Charnley, M.; Goren, T.; Maniura-Weber, K.; Neves, N. M. Differential Regulation of Osteogenic Differentiation of Stem Cells on Surface Roughness Gradients. *Biomaterials* **2014**, *35*, 9023−9032.
(22) Jeon, N. L.; Dertinger, S. K.; Chiu, D. T.; Choi, I. S.; Stroock, A. D.; Whitesides, G. M. Generation of Solution and Surface Gradients Using Microfluidic Systems. *Langmuir* **2000**, *16*, 8311−8316.
(23) Keenan, T. M.; Folch, A. Biomolecular Gradients in Cell Culture Systems. *Lab Chip* **2008**, *8*, 34−57.
(24) Toh, A. G.; Wang, Z. P.; Yang, C.; Nguyen, N. T. Engineering Microfluidic Concentration Gradient Generators for Biological Applications. *Microfluid. Nanofluid.* **2014**, *16*, 1−18.
(25) Zhou, B.; Xu, W.; Wang, C.; Chau, Y.; Zeng, X.; Zhang, X.; Wen, W. Generation of Tunable and Pulsatile Concentration Gradients via Microfluidic Network. *Microfluid. Nanofluid.* **2015**, *18*, 175−184.
(26) Fukumori, K.; Akiyama, Y.; Yamato, M.; Kobayashi, J.; Sakai, K.; Okano, T. Temperature-responsive Glass Coverslips with an Ultrathin Poly(N-isopropylacrylamide) Layer. *Acta Biomater.* **2009**, *5*, 470−476.
(27) Sun, T.; Qing, G. Biomimetic Smart Interface Materials for Biological Applications. *Adv. Mater.* **2011**, *23*, H57−H77.
(28) Stanton, M. M.; Lambert, C. R. A Thermoresponsive, Micro-roughened Cell Culture Surface. *Acta Biomater.* **2015**, *15*, 11−19.
(29) Cooperstein, M. A.; Canavan, H. E. Biological Cell Detachment from Poly(N-isopropyl acrylamide) and Its Applications. *Langmuir* **2009**, *26*, 7695−7707.
(30) Kuroki, H.; Tokarev, I.; Minko, S. Responsive Surfaces for Life Science Applications. *Annu. Rev. Mater. Res.* **2012**, *42*, 343−372.
(31) Quake, S. R.; Scherer, A. From Micro- to Nanofabrication with Soft Materials. *Science* **2000**, *290*, 1536−1539.
(32) Chung, S.; Im, Y.; Choi, J.; Jeong, H. Microreplication Techniques using Soft Lithography. *Microelectron. Eng.* **2004**, *75*, 194−200.
(33) Hu, S.; Ren, X.; Bachman, M.; Sims, C. E.; Li, G. P.; Allbritton, N. Surface Modification of Poly(dimethylsiloxane) Microfluidic Devices by Ultraviolet Polymer Grafting. *Anal. Chem.* **2002**, *74*, 4117−4123.
(34) Wang, X.; McCord, M. G. Grafting of Poly(N-isopropylacrylamide) Onto Nylon and Polystyrene Surfaces by Atmospheric Plasma Treatment Followed with Free Radical Graft Copolymerization. *J. Appl. Polym. Sci.* **2007**, *104*, 3614−3621.
(35) Yu, Q.; Zhang, Y.; Chen, H.; Zhou, F.; Wu, Z.; Huang, H.; Brash, J. L. Protein Adsorption and Cell Adhesion/Detachment Behavior on Dual-Responsive Silicon Surfaces Modified with Poly(N-isopropylacrylamide)-block-polystyrene Copolymer. *Langmuir* **2010**, *26*, 8582−8588.
(36) Wang, Y.; Lai, H. H.; Bachman, M.; Sims, C. E.; Li, G. P.; Allbritton, N. L. Covalent Micropatterning of Poly(dimethylsiloxane) by Photografting through a Mask. *Anal. Chem.* **2005**, *77*, 7539−7546.
(37) Schneider, M. H.; Willaime, H.; Tran, Y.; Rezgui, F.; Tabeling, P. Wettability Patterning by UV-Initiated Graft Polymerization of Poly(acrylic acid) in Closed Microfluidic Systems of Complex Geometry. *Anal. Chem.* **2010**, *82*, 8848−8855.

DOI: 10.1021/acsami.5b04032
ACS Appl. Mater. Interfaces 2015, 7, 17181−17187